Communication

Method to Estimate Antenna Mode Radar Cross Section of Large-Scale Array Antennas

Lei Gan, Wen Jiang, Qiang Chen, Xiaoqiu Li, Zhipeng Zhou, and Shuxi Gong

***Abstract*— A method to estimate the antenna mode radar cross section (AM-RCS) of a large-scale array antenna is proposed. The scattering pattern multiplication method (SPMM) indicates that the antenna mode scattering field of an array antenna can be obtained by the superposition of all the element mode scattering patterns (EMSPs). However, the mutual coupling and edge effects are ignored in the SPMM, which degrades the accuracy. The active element mode scattering pattern (AEMSP) is the EMSP affected by the mutual coupling and edge effects, which is used to improve the SPMM. Furthermore, based on the assumption that the interior elements of a large-scale array antenna have the same array environment as the middle element of its subarray, the proposed method can deduce the AM-RCS of a large-scale array antenna from the subarray. In addition, the accuracy of the proposed method can be improved with the increase of the subarray size. For verifying the generality and reliability, the proposed method is used to estimate the co-polarization AM-RCS of a 21-element microstrip linear array and 15 × 13 Vivaldi planar array. Compared with the reference method, the proposed method has a low calculated error and saves a lot of memory requirement.**

***Index Terms*— Active element pattern (AEP), antenna mode radar cross section (AM-RCS), array antenna, embedded element pattern, scattering pattern multiplication method (SPMM).**

I. Introduction

Phased array antennas have the complex scattering characteristic due to the large number of elements, complicate feed network, and prominent placement [1]. Different from general scatterers, the antenna mode radar cross section (AM-RCS) is unique to the antenna, which is particularly important in the high-gain phased array antenna terminated with the nonideal matched load (ML) [2], [3]. The AM-RCS estimation of a large-scale array antenna is the premise of its stealth design. Therefore, an efficient method to estimate the AM-RCS is essential for evaluating the stealth performance of a large-scale array antenna.

Nowadays, full wave simulation software has become the main tool to evaluate the scattering characteristics of targets such as HFSS, CST, and FEKO [4]. However, for a large-scale array antenna, it is hard to use full wave simulation software to calculate its RCS directly due to the great demand of the computer resources. In this case, it is necessary to propose the AM-RCS estimation method to facilitate the stealth design of a large-scale array antenna. Considering that the radiation field of the array antenna is the product of the array factor and element factor, its scattering field can also be expressed in a similar way, as in [5]. The monostatic scattering pattern multiplication method (SPMM) is a simple and fast method to analyze the monostatic RCS (MRCS) of an array antenna, and it is convenient to optimize the MRCS pattern [6]. The SPMM has a fast computation speed owing to ignoring the mutual coupling and edge effects of an array antenna. However, the mutual coupling effects can greatly affect the performance of array antennas [7]. For example, the gain bandwidths of the large and small arrays are different because of the different mutual coupling effects [1]. In addition, the edge diffraction field is an important factor related to the array antenna pattern, especially for the dual-polarized small array antenna [8], [9]. Therefore, the SPMM needs to be improved through taking mutual coupling and edge effects into account.

The active element pattern (AEP) method, also called the embedded element pattern method, emerges as the times require, which is employed to estimate the radiation pattern of an array antenna [10]–[12]. Under the influence of the surrounding elements, the element radiation pattern in the array deviates from the ideal pattern [8]. Calculated by the numerical algorithm [13], simulated by the full wave simulation software [14], or measured by the microwave anechoic chamber [10], [16], the element in the array environment would behave the AEP, which is an alternative form of the active impedance [10]. In fact, only the adjacent elements of the array antenna have a great effect on the AEP, and other elements do a little. Consequently, a small array, called subarray in [17] and [18], is used to simulate the environment of the large array. Considering the difference of mutual coupling between a large array and subarray, the subarray size has a great effect on estimation efficiency and accuracy. The AEP method is applied in a pyramidal conformal antenna array to estimate its radiation pattern [19], [20]. Generally speaking, the method to solve the radiation problem could be extended to the scattering problem. The frequency selective surfaces [1], perfectly conducting strip arrays [21], [22], and planar slot arrays [23] are taken as examples to prove that the similar concept is suitable for solving scattering problems. In [25], the active element scattering pattern of the central element is obtained through subtracting the M-element array scattering pattern from the $(M + 1)$-element array scattering pattern, and it provides the way to estimate the scattering field of a large-scale array at the cost of a little memory requirement. The antenna mode scattering field (AM-SF) is the reradiating field excited by the energy reflected by the antenna load [1]. Therefore, the AM-SF has the same normalized pattern with the radiation field [26], and the AEP method is naturally extended to the AM-SF calculation.

This communication aims to propose the method to reduce the memory requirement for calculating the AM-RCS of a large-scale array antenna. First, the basis of the proposed method is the SPMM that does not consider the mutual coupling and edge effects. Second, referring to the AEP method in the radiation problem, a method to extract the scattering pattern of elements in an array environment is proposed, named the active element mode scattering pattern

Manuscript received October 23, 2020; revised March 6, 2021; accepted March 21, 2021. Date of publication April 30, 2021; date of current version October 6, 2021. *(Corresponding author: Wen Jiang.)*

Lei Gan, Wen Jiang, Qiang Chen, and Shuxi Gong are with the National Key Laboratory of Science and Technology on Antennas and Microwaves, Xidian University, Xi'an 710071, China (e-mail: lgan123@stu.xidian.edu.cn; jw13@vip.qq.com; chenq@ecei.tohoku.ac.jp).

Xiaoqiu Li and Zhipeng Zhou are with the Science and Technology on Antenna and Microwave Laboratory, Nanjing Research Institute of Electronics Technology, Nanjing 210039, China (e-mail: xqiu12@126.com; 13705174356@139.com).

Color versions of one or more figures in this communication are available at https://doi.org/10.1109/TAP.2021.3075536.

Digital Object Identifier 10.1109/TAP.2021.3075536

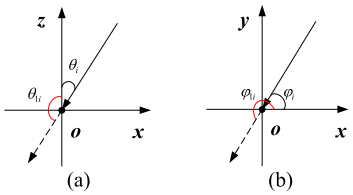

Fig. 1. Incident angle $(\theta_{1i}, \varphi_{1i})$ in the (a) imaginary coordinate system and (b) antenna coordinate system.

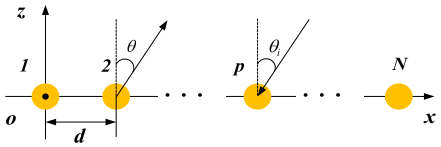

Fig. 2. Uniform linear array composed of N scattering point sources.

(AEMSP) method. Third, the AEMSPs of the interior elements of a large-scale array antenna are approximately the same as that of the middle element of the subarray, which results in that the AM-RCS of the large array antenna can be deduced from the subarray. Therefore, the AM-RCS calculation of a large-scale array antenna can be transformed into each AEMSP calculation in the subarray, thus greatly reducing the memory requirement.

II. Method for Estimating AM-RCS

A. Bistatic SPMM

In the scattering problem, the incident angle (θ_i, φ_i) of a plane wave does not consider the incident direction and is defined in an imaginary coordinate system, while the observation angle (θ, φ) is defined in the antenna coordinate system. Without loss of generality, the incident angle $(\theta_{1i}, \varphi_{1i})$ is defined in the antenna coordinate system, as shown in Fig. 1, that is

$$\begin{aligned} \theta_{1i} &= \pi - \theta_i \\ \varphi_{1i} &= \pi + \varphi_i. \end{aligned} \tag{1}$$

Fig. 2 shows a uniform linear array composed of N scattering point sources arranged on the x-axis, and the element spacing in the array is d. The linear array is excited by an incident plane wave of unit amplitude at an incident angle of θ_i. It is assumed that the magnitude and initial phase of the induced current generated by the pth element are 1 and 0, respectively. The induced current of the pth element can be expressed as

$$I_p = \exp\left[jk\,(p-1)\,d\sin\theta_i\right] \tag{2}$$

where k is the propagation constant of free space. Without special label, E_s is the normalized scattering field when all ports of the array antenna are terminated with the open loads (OLs)

$$E_s = \sum_{p=1}^{N} I_p \exp\left[jk\,(p-1)\,d\sin\theta\right]. \tag{3}$$

The normalized RCS σ_s can be expressed as

$$\sigma_s = \lim_{R\to\infty} 4\pi R^2 \left| \sum_{p=1}^{N} \exp\left[jk\,(p-1)\,d\,(\sin\theta + \sin\theta_i)\right] \right|^2. \tag{4}$$

Equation (4) is the bistatic SPMM. When the incident angle is equal to the observation angle, (4) becomes the monostatic SPMM. However, the mutual coupling and edge effects would affect greatly the accuracy of the SPMM.

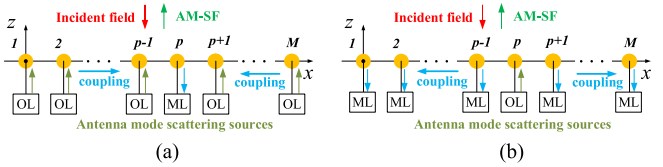

Fig. 3. AM-SF of the N-element linear array on the (a) state 1 and (b) state 3.

B. AEMSP Method

As the same as a general scatterer, the antenna can scatter energy into space, but it also receives a part of the energy at the same time. The received energy would be reflected by the load that is composed of the amplifier, phase shift, and other radio frequency devices terminated by the antenna, and then the antenna excited by the reflected energy would produce the reradiation field, which is the AM-SF that does not exist in general scatterers. Therefore, the total scattering field of antennas contains two components: the AM-SF and structural mode scattering field (SM-SF). The AM-SF is related to the radiation field and loads of antennas, so it does matters for a high-gain array antenna terminated with the nonideal ML.

The SPMM can be used to estimate the AM-SF of array antennas. Assuming that the normalized antenna mode scattering pattern of the pth element is $f_p(\theta, \theta_i)$, the normalized AM-SF E_{as} generated by the linear array terminated with the OLs can be expressed as

$$E_{\text{as}} = \sum_{p=1}^{N} f_p\,(\theta, \theta_i) \exp\left[jk\,(p-1)\,d\,(\sin\theta + \sin\theta_i)\right]. \tag{5}$$

However, the mutual coupling and edge effects of array antennas are not considered in (5). The radiation pattern including mutual coupling and edge effects information is called the active or embedded element pattern [10], and the AM-SF is closely related to the radiation field, so the EMSP in array environment can be called the AEMSP. It is assumed that E_p represents the pth AEMSP in the array, and then E_{as} is

$$E_{\text{as}} = \sum_{p=1}^{N} E_p. \tag{6}$$

Equation (6) represents the AEMSP method.

C. Method to Estimate the Large-Scale Array Antenna

The SM-SF is the total scattering field produced by the antenna terminated with the ML, and the AM-SF is the part of the total scattering field in which the SM-SF is removed [2]. The scattering fields of the array antenna on four states are defined as follows: 1) the scattering field Eo_M^p of the subarray on the state 1 that the pth element is terminated with the ML and others are terminated with the OLs, as shown in Fig. 3(a); 2) the scattering field Eo_M of the subarray on the state 2 that all elements are terminated with the OLs; 3) the scattering field Em_M^p of the subarray on the state 3 that the pth element is terminated with the OL and others are terminated with the MLs, as shown in Fig. 3(b); and 4) the scattering field Em_M of the subarray on the state 4 that all elements are terminated with the MLs.

Obviously, the pth AEMSP can be obtained by $Eo_M - Eo_M^p$. However, a part of energy that is reflected by the OL would be absorbed by the MLs due to the mutual coupling in the array, as shown in Fig. 3(a). On the contrary, the energy that should be absorbed by the ML would be reflected by the OLs, as shown in Fig. 3(b). By calculating the mean value of the two AEMSPs, the error in the scattering problem caused by mutual coupling is

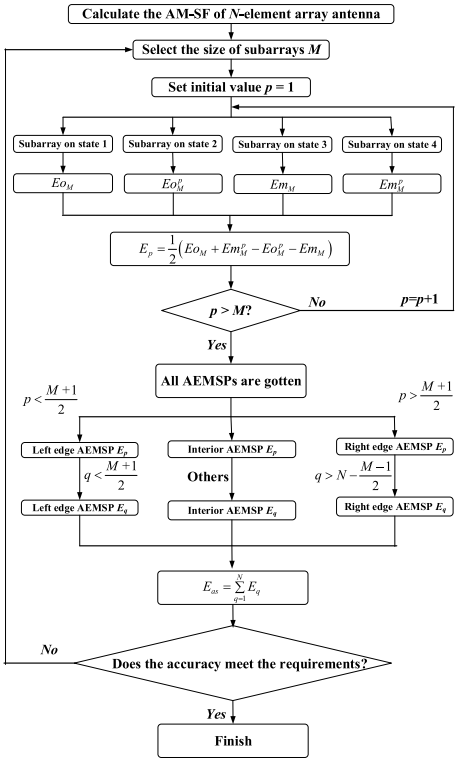

Fig. 4. Flowchart of the proposed method.

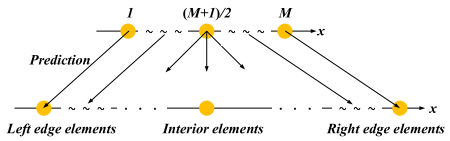

Fig. 5. Method to estimate the AM-RCS of a large-scale array antenna based on the AEMSPs extracted from the M-element subarray.

decreased. When the array number is large enough, the AEMSPs of the interior elements of the array antenna are similar. Consequently, all AEMSPs extracted from the subarray can be used to deduce the AM-SF of a large-scale array antenna. The flowchart of the proposed method is depicted in Fig. 4. The M-element subarray models in four states are established, and the total scattering field is calculated by full wave simulation software. The pth AEMSP is calculated by

$$E_p = \left(Eo_N + Em_N^p - Eo_N^p - Em_N\right)/2. \tag{7}$$

Fig. 5 demonstrates the method to estimate the large-scale array antenna based on the AEMSPs extracted from the M-element subarray. The M-element subarray is used to estimate the AM-RCS of the N-element array antenna ($N > M$). Assuming M is an odd number, the edge AEMSPs in M-element subarray are the same as those in the N-element array antenna, and the $[(M+1)/2]$th AEMSP in the M-element subarray is the same as the other AEMSPs in the N-element array antenna. The AM-SF of the N-element array antenna can be deduced from the M-element subarray by

$$\begin{aligned} E_{\text{as}} = & \sum_{p=1}^{(M+1)/2-1} E_p + \sum_{p=1}^{N-M} E_{(M+1)/2} \\ & \times \exp\left[jk\,(p-1)\,d\,(\sin\theta + \sin\theta_i)\right] + \sum_{p=(M+1)/2+1}^{M} E_p \\ & \times \exp\left[jk\,(N-M)\,d\,(\sin\theta + \sin\theta_i)\right]. \end{aligned} \tag{8}$$

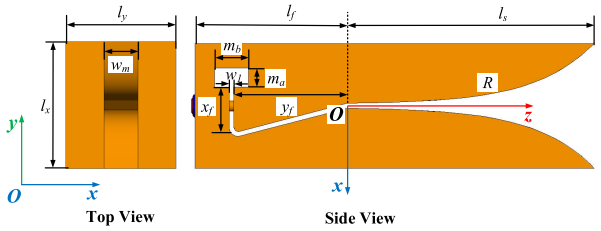

Fig. 6. Geometry of a metal Vivaldi element antenna.

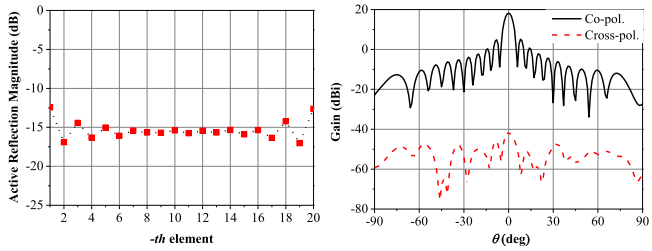

Fig. 7. Performance of 20-element Vivaldi linear array antenna at 10 GHz. (a) Magnitude of each element's active reflection coefficient. (b) Co- and cross-polarization gain of the array antenna on xoz plane.

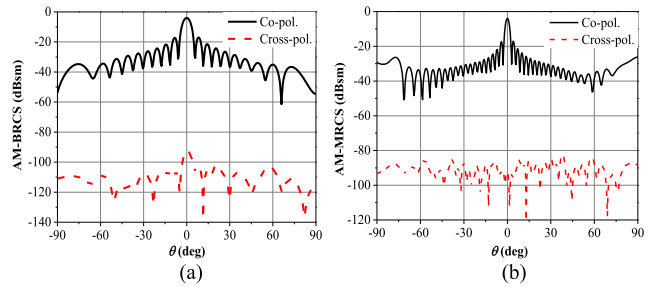

Fig. 8. Co- and cross-polarization AM-RCS patterns of the 20-element Vivaldi array antenna on xoz plane at 10 GHz. (a) AM-BRCS under an x-polarized plane wave incident along $\theta = 0°$. (b) AM-MRCS under an x-polarized plane wave incident along $\theta = (-90° \sim 90°)$.

The AM-SF of the N-element linear array with arbitrary load is

$$E_{\text{as}}(\Gamma_l) = \left[\Gamma_l\right]\left[1 - \Gamma_l\Gamma_a\right]^{-1}\left[1 - \Gamma_o\Gamma_a\right]\left[\Gamma_o\right]^{-1} E_{\text{as}} \tag{9}$$

where Γ_o, Γ_l, and Γ_a are the reflection coefficients of the OL, load, and antenna port, respectively.

D. Accuracy of the Proposed Method

The accuracy of the proposed method is closely related to the size of the subarray. The tradeoff between the accuracy and efficiency of the proposed method needs to be analyzed by practical examples. The geometry of a metal Vivaldi element antenna is shown in Fig. 6. The bottom of Vivaldi antenna is a metal reflector with the size of $l_x \times l_y$, and the element spacing along x-direction is l_x. The coaxial line feeds on the upper wall of the slot line, and a groove with the size of $m_a \times m_b$ is used to reduce the return loss. The formula of the tapered slot is

$$x = \pm\, c_1 \times \exp(0.14z) \pm c_2 \quad (0 \le z \le l_s) \tag{10}$$

where $c_1 = 0.11$ mm, $c_2 = 0.18$ mm. Other parameters of the proposed Vivaldi antenna are described in Table I. The performance of 20-element Vivaldi linear array antenna on xoz plane at 10 GHz is shown in Fig. 7. The active reflection magnitude of the Vivaldi linear array antenna is less than -12.4 dB, and the co- and cross-polarization maximum gain reaches 18.2 and 41.5 dBi, respectively. The co-polarization normalize antenna mode bistatic RCS

TABLE I

PARAMETERS OF THE PROPOSED VIVALDI ANTENNA

Parameters	l_f	l_s	l_x	l_y	m_a
Value/mm	13.2	30	15	13	2.3
Parameters	m_b	w_m	w_1	x_f	y_f
Value/mm	4.1	4	0.58	3.4	13.2

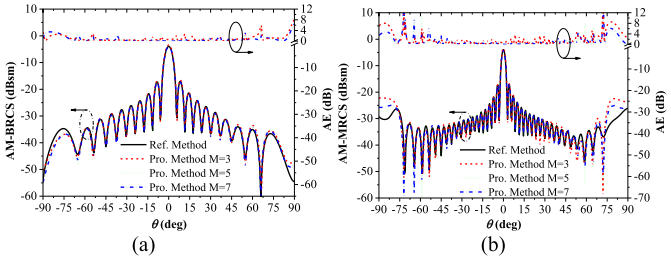

(a) (b)

Fig. 9. With the increase of subarray size M, co-polarization AM-RCS patterns of the 20-element Vivaldi linear array antenna on xoz plane estimated by proposed methods and their AEs compared with the results calculated by the reference method, as increasing the subarray size M. (a) AM-BRCS under an x-polarized plane wave incident along $\theta = 0°$. (b) AM-MRCS under an x-polarized plane wave incident along $\theta = (-90° \sim 90°)$.

(AM-BRCS) pattern has almost the same as the normalized radiation pattern, as shown in Fig. 8. The co- and cross-polarization maximum AM-BRCS reaches −3.9 and −92.3 dBsm, respectively. The co- and cross-polarization maximum antenna mode monostatic RCS (AM-MRCS) reaches −3.9 and −82.3 dBsm, respectively. Theoretically, an ideal linearly polarized antenna has no cross-polarization AM-RCS. Consequently, the co-polarization AM-RCS is used to evaluate the performance of the proposed method.

The co-polarization AM-RCS patterns of the 20-element Vivaldi linear array antenna on xoz plane estimated by proposed methods and their absolute errors (AEs) compared with the results calculated by the reference method are shown in Fig. 9. The AE is the absolute value of the difference between the co-polarization AM-RCS calculated by the reference method and that calculated by the proposed method. It can be seen that the AEs of the co-polarization AM-RCS decrease gradually as the subarray size M increasing from 3 to 7, and it becomes worse at the zero points of the co-polarization AM-RCS patterns. Ignoring the error caused by the zero points, when M is equal to 7, the AE of co-polarization AM-BRCS is less than 1 dB between −71° and 85°, and that of co-polarization AM-MRCS is less than 1 dB between −50° and 52.5°. It can be predicted that increasing the subarray size M can further improve the accuracy, but it would increase the calculation time. Compared with the reference method, the relative error (RE) of the AM-RCS calculated by the proposed method is defined as

$$\mathrm{RE} = \sqrt{\sum_{-\theta}^{+\theta} \left(\sigma_{\mathrm{pro}} - \sigma_{\mathrm{ref}}\right)^2 \Big/ \sum_{-\theta}^{+\theta} \sigma_{\mathrm{ref}}^2} \times 100\% \tag{11}$$

where σ_{pro} and σ_{ref} are AM-RCSs of the 20-element Vivaldi linear array antenna calculated by the proposed method and reference method, respectively. In order to clarify the relationship between calculation accuracy and time of the proposed method, when the subarray size M changes from 3 to 7, the comparison of the calculation resources and the RE of the proposed method is shown in Table II. It can be observed from Table II that with the increase of M, the memory and time requirement of the proposed method increase gradually. When M reaches 7, the time requirement of the proposed method is close to that of the reference method, and the AEs of the proposed method to calculate co-polarization AM-BRCS and

TABLE II

COMPARISON OF THE CALCULATION RESOURCES AND RELATED ERROR FOR THE DIFFERENT SUBARRAY SIZES

		Memory/GByte	Time/hours	RE/%
AM-BRCS	Ref. Method	22.6	6.7	-
	Pro. Method $M = 3$	0.5	0.6	16.1
	Pro. Method $M = 5$	1.4	2.2	6.3
	Pro. Method $M = 7$	2.8	6.3	0.8
AM-MRCS	Ref. Method	22.6	8.6	-
	Pro. Method $M = 3$	0.5	0.9	16.5
	Pro. Method $M = 5$	1.4	3.4	6.3
	Pro. Method $M = 7$	2.8	7.3	1.7

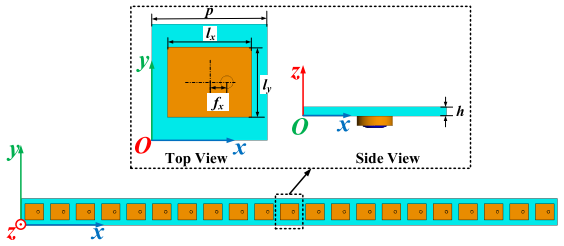

Fig. 10. Geometry of 21-element microstrip patch linear array antenna.

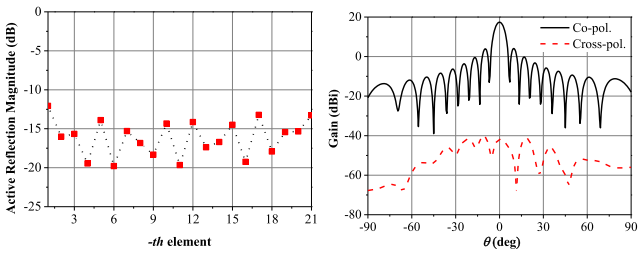

(a) (b)

Fig. 11. Performance of 21-element microstrip linear array antenna at 10 GHz. (a) Magnitude of each element's active reflection coefficient. (b) Co- and cross-polarization gain of the array antenna on xoz plane.

AM-MRCS are 0.8% and 1.7%, respectively. In addition, the memory requirement of the proposed method is 2.8 GB which is only 12% of that of the reference method. Therefore, the proposed method can significantly decrease the memory requirement, and it allows to appropriately select the size of subarrays based on the accuracy and time requirements of practical problems.

III. NUMBER EXAMPLE

In order to ensure that the proposed method is suitable for arbitrary array antennas, two examples are selected to verify the generality and reliability of the proposed method. A 21-element microstrip patch linear array antenna is shown in Fig. 10. The patch with the size of $l_x \times l_y$ (8.8×7.2 mm^2) is placed on the dielectric substrate with the dielectric constant of 2.2 and thickness of $h = 1$ mm. The feed position deviates from the y-axis $f_x = 1.8$ mm. The microstrip array antenna operates at 10 GHz and the element spacing p is 12 mm. The performance of the 21-element microstrip patch linear array antenna on xoz plane at 10 GHz is shown in Fig. 11. Fig. 11(a) indicates that the active reflection magnitude of the microstrip linear array antenna is less than −12.1 dB. Fig. 11(b) shows that the co-polarization gain peak reaches 17.3 dBi, and its cross-polarization ratio is 58.9 dB. The AEMSPs of 7-element subarray are used to deduce the co-polarization AM-RCS of 21-element linear array antenna. The co-polarization AM-RCS patterns of 21-element microstrip patch linear array antenna on xoz plane estimated by the proposed method and SPMM are shown in Fig. 12. Compared with the reference method, the amplitude of the co-polarization AM-RCS estimated by

TABLE III
COST AND ERROR OF THE AM-RCS PATTERN ESTIMATED BY THE PROPOSED METHOD

		AM-BRCS			AM-MRCS		
		Memory/GByte	Time/hours	RE/%	Memory/GByte	Time/hours	RE/%
Ref. Method	20-element Vivaldi linear array	22.6	6.8	-	22.6	8.8	-
	21-element microstrip linear array	6.6	5.6	-	25.5	22.5	-
	15×13 Vivaldi planar array	650.3	763	-	650.3	770	-
SPMM	20-element Vivaldi linear array	<0.1	2	-	<0.1	2	-
	21-element microstrip linear array	<0.1	8.7	32.7	<0.1	8.7	34.5
	15×13 Vivaldi planar array	<0.1	2	7.1	<0.1	2	7.1
Pro. Method	20-element Vivaldi linear array	2.8	6.4	0.8	2.8	7.9	1.7
	21-element microstrip linear array	0.2	1.2	0.6	0.2	12.1	1.5
	15×13 Vivaldi planar array	36.4	374.8	0.7	36.4	320	2.4

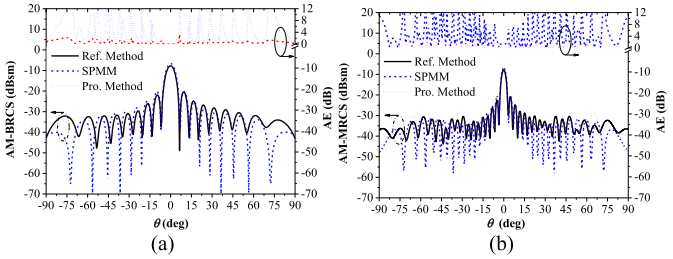

Fig. 12. Co-polarization AM-RCS patterns of the 21-element microstrip patch linear array antenna on *xoz* plane estimated by the proposed method and SPMM, and their AEs compared with the results calculated by the reference method. (a) AM-BRCS under an x-polarized plane wave incident along $\theta = 0°$. (b) AM-MRCS under an x-polarized plane wave incident along $\theta = (-90° \sim 90°)$.

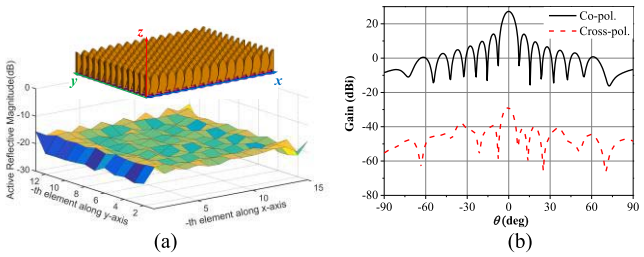

Fig. 13. Performance of 15 × 13 Vivaldi planar array antenna at 10 GHz. (a) Magnitude of each element's active reflection coefficient. (b) Co- and cross-polarization gain of the array antenna on *xoz* plane.

SPMM is slightly high, and the co-polarization AM-RCS patterns estimated by the proposed method are almost the same as that calculated by the reference method. However, near grazing incidence direction, the value and position of the peak and valley are slightly shifted, and especially the AEs of the co-polarization AM-MRCS estimated by the proposed method deteriorate seriously. Ignoring the error caused by the peak and valley points, the AEs of the co-polarization AM-BRCS are less than 1 dB between −70.5° and 69°, and those of the co-polarization AM-MRCS are less than 1 dB between −60.5° and 54.5°.

The proposed method can also be extended to estimate the co-polarization AM-RCS of a planar array antenna. A 15 × 13 Vivaldi planar array antenna with half wavelength element spacing is designed. The element structure parameters are the same as those in Fig. 6, and its performance is shown in Fig. 13. Fig. 13(a) indicates that the active reflection magnitude of the Vivaldi planar array antenna is less than −15.3 dB. Fig. 13(b) shows that the co-polarization gain peak reaches 27.2 dBi, and its cross-polarization ratio is 55.9 dB. The AEMSPs of the 7 × 7 metal Vivaldi subarray antenna are calculated, and then they are used to deduce the co-polarization AM-RCS of the Vivaldi

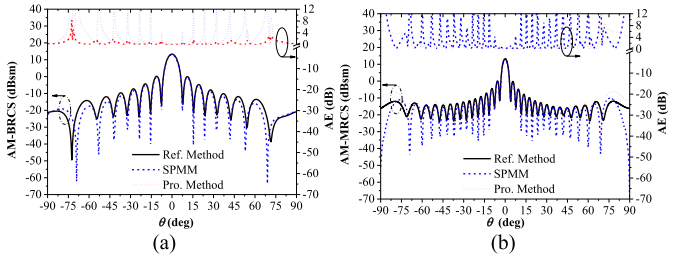

Fig. 14. Co-polarization AM-RCS patterns of the Vivaldi planar array antenna on *xoz* plane estimated by the proposed method and SPMM, and their AEs compared with the results calculated by the reference method. (a) AM-BRCS under an x-polarized plane wave incident along $\theta = 0°$. (b) AM-MRCS under an x-polarized plane wave incident along $\theta = (-90° \sim 90°)$.

planar array antenna. The co-polarization AM-RCS patterns of the Vivaldi planar array antenna on *xoz* plane estimated by the proposed method and SPMM are shown in Fig. 14. It can be seen that when the scale of the array antenna is enough large, the main lobe of the co-polarization AM-RCS estimated by SPMM is accurate, but the accuracy in other directions is not enough. Ignoring the error caused by the peak and valley points, the AEs of the co-polarization AM-BRCS are less than 1 dB between −68.5° and 68°, and those of co-polarization AM-MRCS are less than 3 dB between −68° and 68° and 1 dB between −30.5° and 39°. Compared with the SPMM, the co-polarization AM-RCS calculated by the proposed method is slightly different from the reference result only when it is close to the grazing incidence direction. The cost and error of the AM-RCS pattern estimated by the proposed method are shown in Table III.

For the 20-element Vivaldi linear array, compared with the reference method, the proposed method saves 88% memory requirement. In addition, the RE of the co-polarization AM-BRCS estimated by the proposed method is 0.8%, and that of the co-polarization AM-MRCS pattern is 1.7%.

For the 21-element microstrip linear array, the REs of the co-polarization AM-BRCS estimated by the SPMM and proposed method are 32.7% and 0.6%, respectively, and those of the co-polarization AM-MRCS estimated by the SPMM and proposed method are 34.5% and 1.5% respectively.

For the 15 × 13 Vivaldi planar array, compared with the reference method, the SPMM saves 99% memory and time requirement, and the proposed method saves 94% memory requirement and 50% computing time. In addition, the REs of the co-polarization AM-BRCS estimated by the SPMM and proposed method are 7.1% and 0.7%, respectively, and those of the co-polarization AM-MRCS estimated by the SPMM and proposed method are 7.1% and 2.4%, respectively.

The calculation error of the SPMM comes from the following two points: 1) the mutual coupling effects of the finite and infinite array antennas are not identical and 2) the edge effect is not considered in

the SPMM. Similar to the AEP method, the AEMSPs extracted from the subarray contain the mutual coupling and edge effects. Based on the assumption that the middle element antenna of subarray has the same array environment as the interior element antennas of a large array antenna, the proposed method uses the AEMSPs to synthesize the AM-RCS pattern of the large array antenna. Compared with the SPMM, the proposed method improves the calculation accuracy of the AM-RCS at the cost of a little memory requirement increasing.

IV. Conclusion

This communication proposes a method to estimate the AM-RCS of a large-scale array antenna, and it alleviates the computer memory requirements. The SPMM is the basis of the proposed method, but it considers the mutual coupling and edge effects insufficiently. Similar to the AEP method, the AEMSP represents the EMSP including the mutual coupling and edge effects. The AM-RCS pattern of an array antenna can be synthesized by the superposition of all AEMSPs in the array antenna. Furthermore, based on the assumption that the middle element pattern of subarray has the same array environment as the interior element patterns of a large array antenna, the proposed method can deduce the AM-RCS of a large-scale array antenna from a small array antenna. The example of a 20-element Vivaldi linear array antenna shows that the larger size of the subarray, the higher accuracy of the proposed method. In addition, a 21-element microstrip linear array and 15×13 Vivaldi planar array are used to prove the reliability and generality of the proposed method. The proposed method can be used to solve the problem of excessive memory requirement in AM-RCS calculation of a large-scale array antenna.

References

[1] R. J. Mailloux, "Phased array theory and technology," *Proc. IEEE*, vol. 70, no. 3, pp. 246–291, Mar. 1982.

[2] B. A. Munk, *Finite Antenna Arrays and FSS*. Piscataway, NJ, USA: IEEE Press, 2003, pp. 17–23.

[3] R. C. Hansen, "Relationships between antennas as scatterers and as radiators," *Proc. IEEE*, vol. 77, no. 5, pp. 659–662, May 1989.

[4] *Altair FEKO*. Altair Engineering, Inc., Troy, MI, USA. [Online]. Available: https://www.altair.com/feko

[5] B. Lu, S.-X. Gong, S. Zhang, and J. Ling, "A new method for determining the scattering of linear polarized element arrays," *Prog. Electromagn. Res. M*, vol. 7, pp. 87–96, May 2009.

[6] B. Lu, S. X. Gong, S. Zhang, Y. Guan, and J. Ling, "Optimum spatial arrangement of array elements for suppression of grating-lobes of radar cross section," *IEEE Antennas Wireless Propag. Lett.*, vol. 9, pp. 114–117, 2010.

[7] J. Allen, "Gain and impedance variation in scanned dipole arrays," *IRE Trans. Antennas Propag.*, vol. 10, no. 5, pp. 566–572, Sep. 1962.

[8] J. A. Ortiz, N. Aboserwal, and J. L. Salazar, "A new analytical model based on diffraction theory for predicting cross-polar patterns of antenna elements in a finite phased array," in *Proc. IEEE Int. Symp. Phased Array Syst. Technol. (PAST)*, Oct. 2019, pp. 1–4.

[9] J. L. Salazar, N. Aboserwal, J. D. Diaz, J. A. Ortiz, and C. Fulton, "Edge diffractions impact on the cross polarization performance of active phased array antennas," in *Proc. IEEE Int. Symp. Phased Array Syst. Technol. (PAST)*, Oct. 2016, pp. 1–5.

[10] D. M. Pozar, "A relation between the active input impedance and the active element pattern of a phased array," *IEEE Trans. Antennas Propag.*, vol. 51, no. 9, pp. 2486–2489, Sep. 2003.

[11] P. Hannan, "The element-gain paradox for a phased-array antenna," *IEEE Trans. Antennas Propag.*, vol. AP-12, no. 4, pp. 423–433, Jul. 1964.

[12] D. M. Pozar, "The active element pattern," *IEEE Trans. Antennas Propag.*, vol. 42, no. 8, pp. 1176–1178, Aug. 1994.

[13] D. F. Kelley and W. L. Stutzman, "Array antenna pattern modeling methods that include mutual coupling effects," *IEEE Trans. Antennas Propag.*, vol. 41, no. 12, pp. 1625–1632, Dec. 1993.

[14] Q.-Q. He and B.-Z. Wang, "Design of microstrip array antenna by using active element pattern technique combining with Taylor synthesis method," *Prog. Electromagn. Res.*, vol. 80, pp. 63–76, Nov. 2008.

[15] B. Y. Toh, V. F. Fusco, and N. B. Buchanan, "Retrodirective array tracking prediction using active element characterisation," *Electron. Lett.*, vol. 37, no. 12, pp. 727–728, Jun. 2001.

[16] E. Ercil, E. Yildirim, and M. E. Inal, "Array antenna pattern synthesis using measured active element patterns and Gram—Schmidt Orthogonalization," in *Proc. IEEE Int. Symp. Phased Array Syst. Technol.*, Waltham, MA, USA, Oct. 2010, pp. 357–360.

[17] S. Zhang, S. Gong, and H. Hu, "A novel active element pattern method for calculation of large linear arrays," in *Proc. Int. Symp. Antennas Propag.*, Nanjing, China, Oct. 2013, pp. 220–222.

[18] S. Zhang, X. Wang, and L. Chang, "Radiation pattern of large planar arrays using four small subarrays," *IEEE Antennas Wireless Propag. Lett.*, vol. 14, pp. 1196–1199, 2015.

[19] X.-S. Yang, H. Qian, B.-Z. Wang, and S. Xiao, "Radiation pattern computation of pyramidal conformal antenna array with active-element pattern technique," *IEEE Antennas Propag. Mag.*, vol. 53, no. 1, pp. 28–37, Feb. 2011.

[20] K. Yang, Z. Zhao, Z. Nie, J. Ouyang, and Q. H. Liu, "Synthesis of conformal phased arrays with embedded element pattern decomposition," *IEEE Trans. Antennas Propag.*, vol. 59, no. 8, pp. 2882–2888, Aug. 2011.

[21] T. Cwik and R. Mittra, "The effects of the truncation and curvature of periodic surfaces: A strip grating," *IEEE Trans. Antennas Propag.*, vol. AP-36, no. 5, pp. 612–622, May 1988.

[22] L. Carin and L. B. Felsen, "Time harmonic and transient scattering by finite periodic flat strip arrays: Hybrid (ray)-(floquet mode)-(MOM) algorithm," *IEEE Trans. Antennas Propag.*, vol. 41, no. 4, pp. 412–421, Apr. 1993.

[23] P. J. Collins and J. P. Skinner, "A hybrid moment method solution for TE/sub z/ scattering from large planar slot arrays," *IEEE Trans. Antennas Propag.*, vol. 50, no. 2, pp. 145–156, Feb. 2002.

[24] D. M. Kokotoff, D. T. Auckland, and J. M. Bornholdt, "A subarray dilation method for computing scattering and radiation from large slot arrays," in *Proc. Int. Symp. Antennas Propag. Soc., Merging Technol.*, Dallas, TX, USA, 1990, pp. 1738–1741.

[25] S. Zhang, S. Gong, Q. Gong, Y. Guan, and B. Lu, "Application of the active element pattern method for calculation of the scattering pattern of large finite arrays," *IEEE Antennas Wireless Propag. Lett.*, vol. 10, pp. 83–86, 2011.

[26] L. Gan, W. Jiang, Q. Chen, X. Li, and Z. Zhou, "Analysis and reduction on in-band RCS of Fabry–Perot antennas," *IEEE Access*, vol. 8, pp. 146697–146706, 2020.